Electronic Supplementary Material (ESI) for Soft Matter.

Supporting Information: Composition and temperature effects on the solution structure of SDS/octanol/brine by SANS, NMR and microscopy

Liva Donina, Lionel Porcar, and João T. Cabral*

October 16, 2023

1 NMR characterisation of pure components SDS and octanol in solution

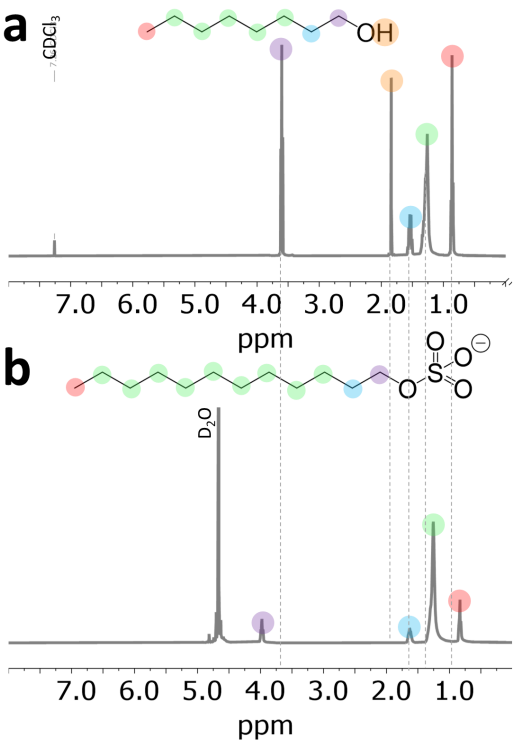

Figure S1: ^{1}H NMR of 6.5 % w/w SDS in D_2O and 7.9 % w/w octanol in $CDCl_3$ at 25 °C

2 SANS model description

2.1 SLD calculations

Scattering length densities (SLD) were estimated following standard procedures, for various oct:SDS ratios, as well as expected dimensions and tilt of surfactant aggregates, as described in Fig. S2.

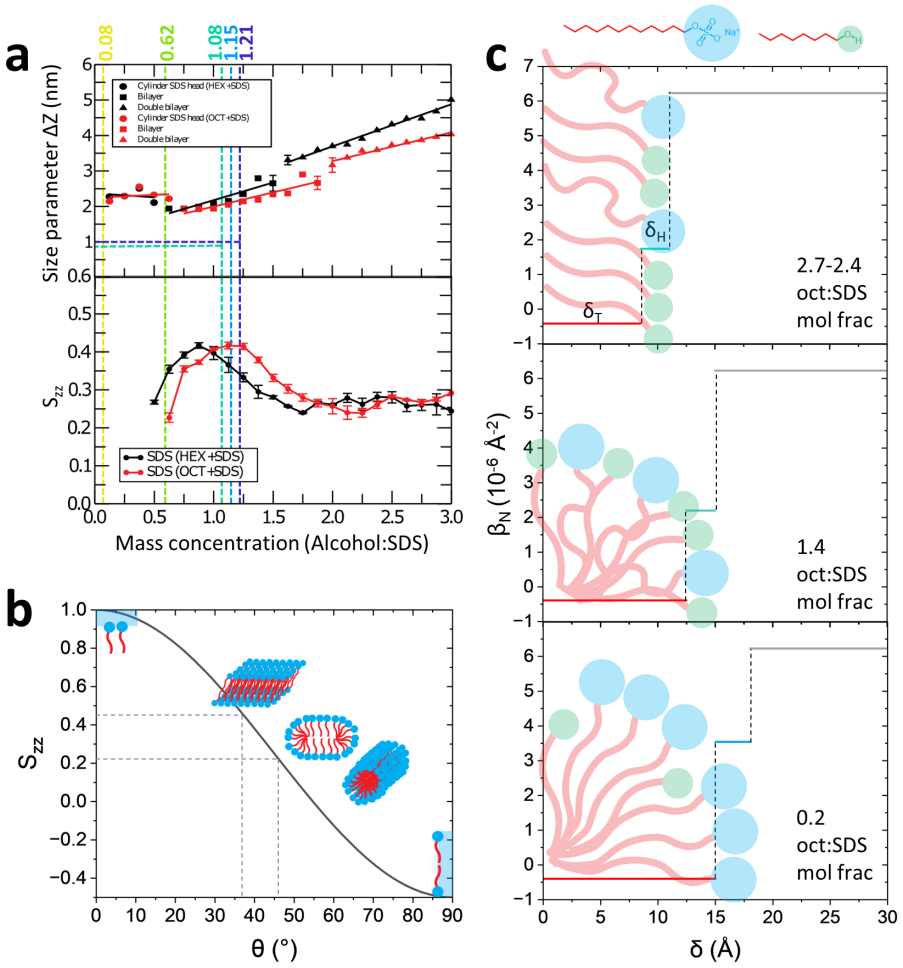

Figure S2: Molecular dimensions and SLDs for samples with oct:SDS ratios of 1.21, 1.15, 1.08, 0.62 and 0.08 a) ΔZ, which corresponds to membrane thickness or micellar radius as a function of octanol concentration (top), S_{zz} parameter as a function of octanol concentration (bottom) describing the surfactant tail tilt, -0.5 corresponds to tails parallel to water interface while 1.0 corresponds to tails normal to water interface, b) Surfactant tail tilt in the systems of interest; c) SLD calculations of lamellar 1.08-1.21 (top), mixed 0.62 (middle) and micellar 0.08 (bottom).

2.2 Structure of SDS/octanol/brine sponge phase L_3

Quantitative description of sponge phase L_3 for the molar octanol:SDS ratio of 0.27 (or 1.21 w/w) was achieved by fitting structure factor $S(q)$ model (1) described by Lei et al. [1],

$$S(q) = 1 + \frac{A \arctan[q\xi_{io}/2]}{q} + \frac{B}{\xi_3^{-2} + (q - q_3)^2} \tag{1}$$

where ξ_{io} is inside/outside correlation length which describes correlation on a large scale much larger than ξ_3 which

describes sponge pore correlation length. q_3 is the position of the Bragg peak (conversely, average sponge pore size is $\xi = 2\pi/q_3$) and A and B are S(q) prefactors. The structure factor is dominated by the second term (prefactor B) because the membrane concentration is relatively small. Porcar et al [2] report ξ_3 of values around 85 Å which are the values we fit for our system.

Analytic approximation describing membrane "discoids" (2)was employed to describe the form factor $P(q)$ [2],

$$P(q) = 4(\pi\sigma^2\Delta\rho)^2 \frac{1 - \cos[qt_0]\exp[-q^2t_0^2/32]/q^2}{q^2\sigma^2 + 2\exp[-q\sigma^2/6]} \tag{2}$$

where σ is the radius of gyration of the discoid, t_0 thickness of membrane's hydrocarbon core, which in this case is between 17-30 Å and $\Delta\rho$ is the neutron contrast between the hydrocarbon tail and solvent has been estimated to be 5.9 $\text{Å}^{-2}10^{-6}$ from the molecular volume. Overall thickness of sponge phase membrane δ is $t_0 + 5$.

The observed coherent scattering I_{coh} is

$$I_{coh}(q) = NS(q)P(q) \tag{3}$$

where $N = \phi_v/\pi\sigma^2\delta$ where ϕ_v is membrane volume fraction calculated as $(V_{octanol} + V_{SDS})/V_{total}$

2.3 Structure of SDS/octanol/brine lamellar phase L_α

Lamellar structures were fitted with a Caillé structure factor model [3] preprogrammed in SASView considering scattering from surfactant head and tail groups separately. The structure factor is given by

$$S(q) = 1 + 2\sum_{n=1}^{N-1}(1 - \frac{n}{N})\cos(q\,dn)\exp(-\frac{2q^2d^2\alpha(n)}{2}) \tag{4}$$

where N is number of lamellar stacks and

$$\alpha(n) = \frac{\eta_{cp}}{4\pi^2}(ln(\pi n) + \gamma_E) \tag{5}$$

with $\eta_{cp} = \frac{q_0^2 k_B T}{8\pi\sqrt{K\overline{B}}}$ being Caillé parameter where K is the membrane bending rigidity $\overline{B}$ is the membrane compression modulus. γ_E is Euler's constant with value of 0.58. The form factor reads

$$P(q) = \frac{4}{q^2}\ {\Delta\rho_H}^2(\sin[q(\delta_H + \delta_T)])^2 - {\Delta\rho_T}^2(\sin(q\delta_T))^2 \tag{6}$$

Where $\Delta\rho_H$ is $SLD_H - SLD_{brine}$ and $\Delta\rho_T$ is $SLD_{tail} - SLD_H$; δ_H is the thickness of the headgroup ($-OH$) and $-SO_4Na$) and δ_T is the hydrocarbon chain of octanol and SDS.

The coherent scattering I_{coh} is given by

$$I(q) = 2\pi\frac{P(q)S(q)}{q^2\delta} \tag{7}$$

We explore the parameter space by varying one parameter as shown in Fig. S2. Since we are working with dilute lamellar phases, broad peaks are often observed. Peak shape is can be described by Caillé parameter eta and d-spacing polydispersity p_D. Fig. S3b shows the effect of the degree of p_D and shows that a degree of polydispersity is required to characterise lamellar phases investigated in this work.

An example fit is given in S4 where the effect of varying p_D and η is shown. This fitting demonstrates the need to vary both p_D and η as the low q region cannot be fitted with varying η alone.

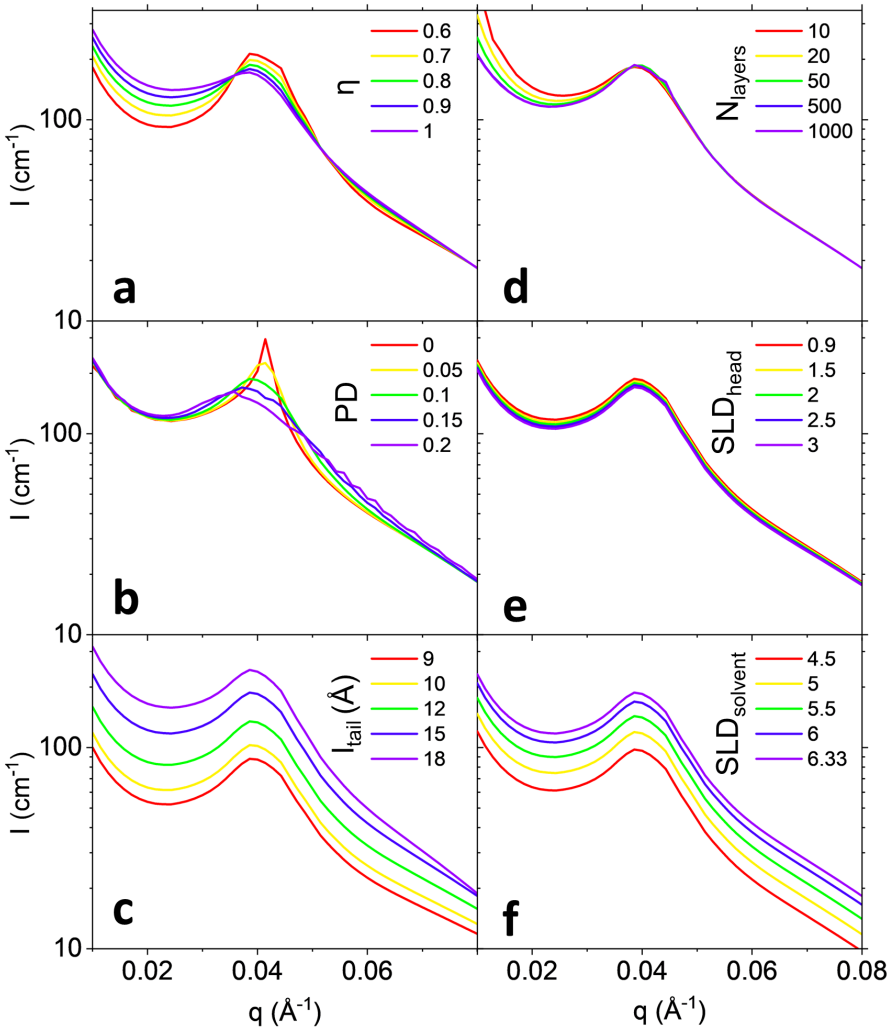

Figure S3: Parameters in Caillé S(q) structure factor model. a) Caillé parameter ($\eta = 0.6 - 1.0$) describing lamellar membrane physical properties; b) Polydispersity of d-spacing ($p_D = 0 - 0.25$) describing Gaussian d-spacing distribution; c) Surfactant hydrocarbon tail length ($l_{tail} = 9 - 18$ Å); d) Number of lamellar stacks ($N_{layers} = 10 - 1000$); e) Scattering length density for the headgroup consisting of $-SO_4$ and $-OH$ ($SLD_{head} = 0.9 - 3$ Å$^{-2}10^{-6}$); f) Scattering length density for the solvent (D_2O and NaCl) ($SLD_{head} = 4.5 - 6.33$ Å$^{-2}10^{-6}$).

Bjerrum length λ_B and Debye length λ_D were calculated to correlate the structural changes observed in the lamellar L_α phase upon increasing temperature and dilution. The Bjerrum length reads

$$\lambda_B = \frac{e^2}{4\pi\epsilon_w\epsilon_0 k_B T} \tag{8}$$

where e is elementary charge, ϵ_w is the dielectric constant of water, ϵ_0 is the vacuum permittivity, k_B is Boltzmann constant and T is temperature in K. At a first glance, one might think that increasing temperature will decrease λ_B. However, ϵ_w decreases with increasing T which will result in overall increase of λ_B with temperature. Addition of an electrolyte will further decrease ϵ_w. The value for ϵ_w in presence of 0.3 M NaCl (concentations of NaCl in solutions used in our study) is 74.5 at 25 °C, lower than that of 78.3 in just water. Empirically, the effect of T on ϵ_w is expected [4] to follow:

$$\epsilon_w(T) = 87.740 - 0.4008T + 9.398 \times 10^{-4}T^2 - 1.410 \times 10^{-6}T^3 \tag{9}$$

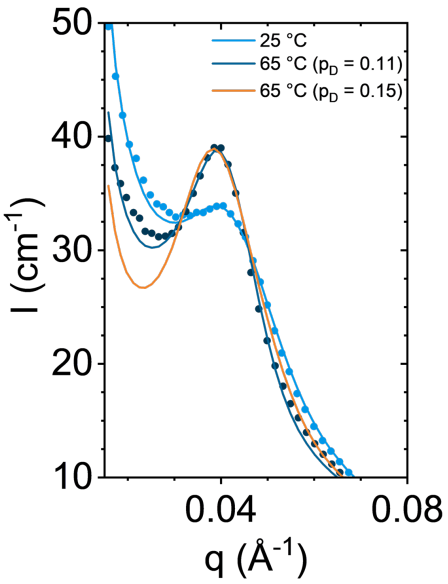

Figure S4: Comparison between polydisperisty p_D values in fitting. p_D=0.15 and Caillé parameter η=1 at 25 °C; p_D = 0.11 and η=0.9 at 65 °C; p_D=0.15 and η = 0.75 at 65 °C.

We obtain the value of 74.5 for ϵ_w at 25 °C in presence of 0.3 M NaCl solution from study by Gavish and Promislow [5] and back-calculation of ϵ_w at 0 °C gives the value of 84.5. λ_B for 0 M and 0.3 M NaCl concentrations as a function of T is given in Fig. S5.

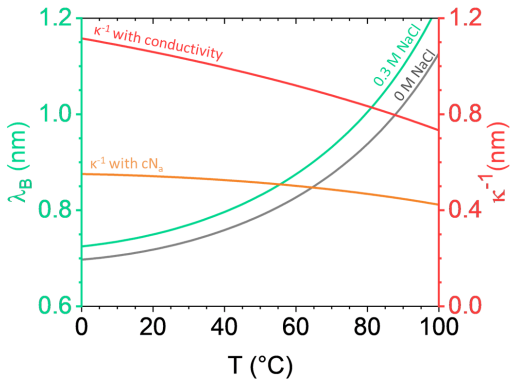

Figure S5: Bjerrum length λ_B and Debye length κ^{-1} as a function of T for 0 M and 0.3 M NaCl concentrations. Temperature effect on λ_B has been calculated for both 0 M and 0.3 M NaCl conditions showing and increase in λ_B with increasing T and NaCl (shown in green and grey lines, κ^{-1} Debye length has been calculated using conductivity approach (red) and from ionic strength (orange) considering only NaCl contributions)

The Debye length in electrolyte solutions is given by

$$\kappa^{-1} = \sqrt{\frac{\epsilon_w \epsilon_0 k_B T}{2e^2 N_a c}} \tag{10}$$

where N_a is Avogadro's constant and c is the concentration of the ionic species.

Alternatively, and perhaps more accurately, the Debye length κ^{-1} can be estimated from K_c measurements (which for the 6.5 % SDS, 7.9 % octanol and 85.6 % brine sample has been measured 10.2 mS/cm) and diffusion constant for Na^+ and Cl^- ions is 1.7 $\mu m^2 ms^{-1}$.

$$\kappa^{-1} = \sqrt{\frac{\epsilon_w \epsilon_0 D}{K_c}} \tag{11}$$

2.4 Structure of SDS/octanol/brine micellar L_{mix} phase

In the mixed phase region between L_1 and L_α we observe exponent $-k$ of $\sim$ 3-4 which is indicative of presence of multilamellar vesicles and elongated micelles. Here, the structures were described as the Caillé structure factor model and flexible cylinder sum. Flexible cylinder model is given by:

$$P(q) = \frac{scale}{V} F^2(q) + I_{incoh} \tag{12}$$

2.5 Structure of SDS/octanol/brine micellar L_1 phase

The addition of salt NaCl and mid-to-long chain 1-alcohol such as 1-octanol favours the formation of wormlike micelles. To describe these structures we fit core shell cylinder model [6] available on SasView. The form factor is given by (7):

$$F(q,\alpha) = (\rho_c - \rho_s) V_c \frac{\sin(q\frac{1}{2}L\cos\alpha)}{q\frac{1}{2}L\cos\alpha} \frac{2J_1(qR\sin\alpha)}{qR\sin\alpha} + (\rho_s - \rho_{solv}) V_s \frac{\sin(q(\frac{1}{2}L+T)\cos\alpha)}{q(\frac{1}{2}L+T)\cos\alpha} \frac{2J_1(q(R+T)\sin\alpha)}{q(R+T)\sin\alpha} \tag{13}$$

and

$$V_s = \pi(R+T)^2(L+2T) \tag{14}$$

where α is the angle between the cylinder and the scattering vector q, ρ_c is the scattering length density of the core, ρ_s is the scattering length density of the shell and ρ_{solv} is the scattering length density of the solvent, V_s is the total volume of the cylinder, V_c is the the volume of the core (8), R is the radius of the core, L in the length of the core and T is the thickness oft the shell. The outer radius is given by $R+T$ and the total length including shell is $L+2T$; J_1 is first order Bessel function.

The coherent scattering is given by (9):

$$I(q,\alpha) = \frac{scale}{V_s} F^2(q,\alpha)\sin(\alpha) + I_{incoh} \tag{15}$$

3 Lamellar phase L_α optical microscopy and SANS

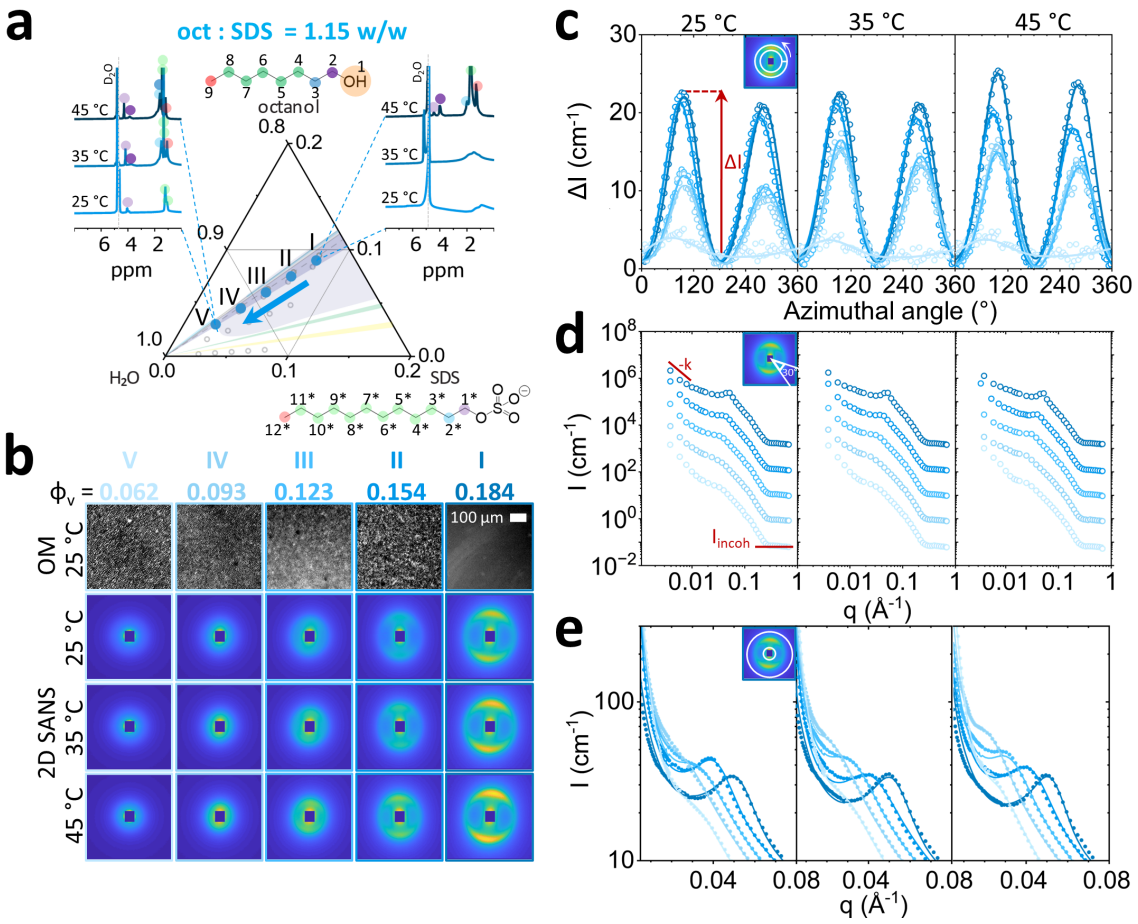

Figure S6: Lamellar phase along the dilution line towards H_2O corner with 1.15 w/w octanol:SDS ratio a) Overview of the experimentally measured compositions at octanol:SDS ratio 1.15, L_α phase region. Specifically, SDS/octanol/H_2O brine: I) 7.8/9.0/82.2, II) 6.5/7.5/86.0, III) 5.2/6.0/88.8, IV) 3.9/4.5/91.6, V) 2.60/3.0/94.4 (prepared from dilution of I); for SANS and NMR samples, D_2O was used instead. Representative NMR spectra are shown for I) and V) as a function temperature. b) Corresponding birefringence and brightfield (BF) optical microscopy data at 25 °C and SANS at 25, 35 and 45 °C of samples I-V; ϕ_v indicates the SDS+octanol volume fraction, i.e. total surfactant/co-surfactant content. c) Azimuthal profile of SANS data in b) around the respective Bragg peak for Δq=0.014 Å^{-1}, subtracted by the respective I_{min} characterising scattering anisotropy. d) Sector average $I(q)$ with a 30° angular range, normal pattern orientation; dashed lines indicate peak position(s). Data shifted vertically ($\times$10) for clarity. e) Radial average of SANS data near the peak; lines are fits to the lamellar model, described in the text.

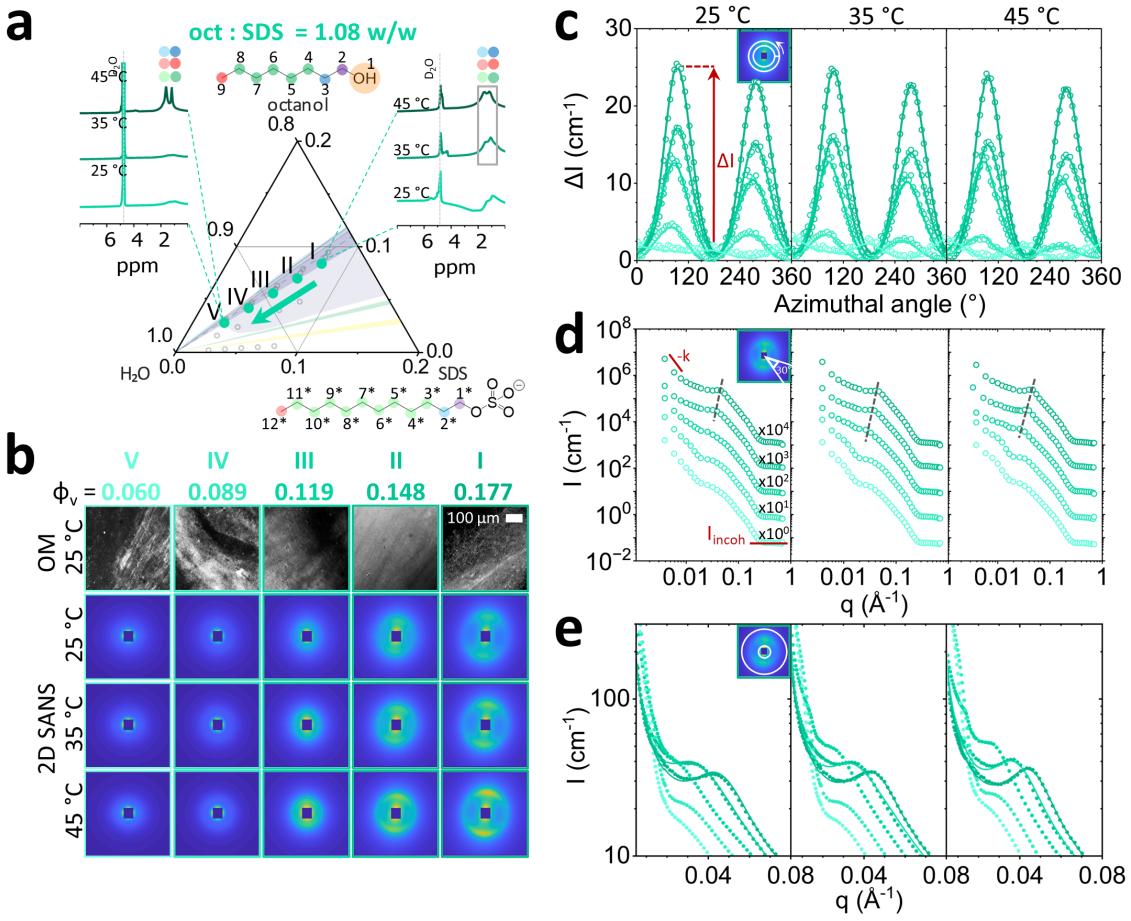

Figure S7: Lamellar phase along the dilution line towards H_2O corner with 1.08 w/w octanol:SDS ratio. a) Overview of the experimentally measured compositions at octanol:SDS ratio 1.08, L_α phase region close to the mixed phase L_α/L_4. Specifically, SDS/octanol/H_2O brine: I) 7.8/8.4/83.8, II) 6.5/7.0/86.5, III) 5.20/5.6/89.2, IV) 3.9/4.2/91.9, V) 2.6/2.8/94.6 (prepared from dilution of I); for SANS and NMR samples, D_2O was used instead. Representative NMR spectra are shown for I) and V) as a function temperature. b) Corresponding birefringence and brightfield (BF) optical microscopy data and SANS of samples I-V at 25, 35 and 45 °C; ϕ_v indicates the SDS+octanol volume fraction, i.e. total surfactant/co-surfactant content. c) Azimuthal profile of SANS data in b) around the respective Bragg peak for Δq=0.014 Å^{-1}, subtracted by the respective I_{min} characterising scattering anisotropy. d) Sector average $I(q)$ with a 30° angular range, normal pattern orientation; dashed lines indicate peak position(s). Data shifted vertically ($\times$10) for clarity. e) Radial average of SANS data near the peak; lines are fits to the lamellar, described in the text.

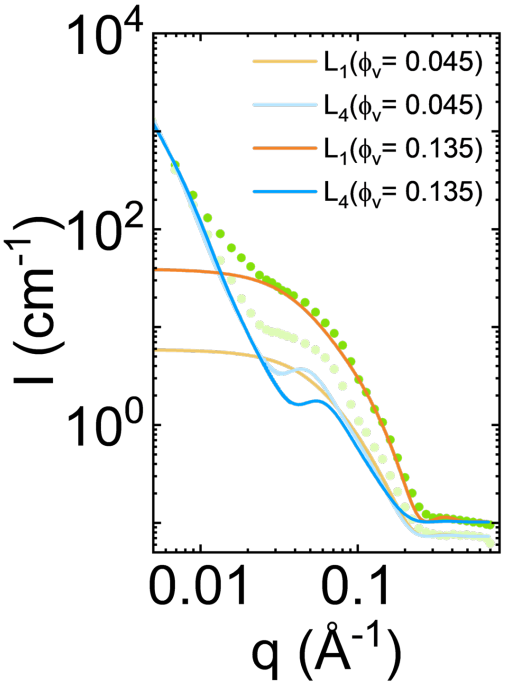

Figure S8: Illustrative L_1/L_4 mixed phase model contributions for samples $\phi_v = 0.045$ and $\phi_v = 0.135$ at 25 °C. Orange colour fits indicate `flexible_cylinder` model contributions for L_1 phase while blue colour fits indicate `lamellar_hg_stack_caille` model contributions for L_4 phase. Overall, with sample dilution, the flexible cylinder model contribution becomes more apparent.

The data span 4 orders of magnitude in absolute intensity, and the models do not strictly apply across the entire q-range. Thus the χ^2 obtained are generally large, and used in relative terms to compare our results.

4 Dilution fitting results at 25°C, 35°C and 45°C

T, °C	ϕ_v	I_{incoh}, cm^{-1}	scale	δ_{tail}, Å	δ_m, Å	N$_{layers}$	d, Å	η	p_D	χ^2
25	0.189	0.121	0.91	8.5±0.1	23.0	1000	128.1±0.3	0.91±0.01	0.08	2044
	0.158	0.109	0.91	9.2±0.1	24.4	2000	150.7±0.3	1.00±0.01	0.10	1870
	0.127	0.099	1.00	9.5±0.1	25.0	1000	199.0±0.3	1.00±0.01	0.19	1850
	0.096	0.064	0.3	9.5±0.1	25.0	1000	273.7±0.3	1.00±0.01	0.22	96
	0.064	0.055	0.45	9.5±0.1	25.0	1000	395.0±0.3	1.00±0.01	0.25	161
35	0.189	0.113	0.90	9.0±0.1	24.0	1000	118.1±0.3	0.75±0.07	0.06	9150
	0.158	0.109	0.35	9.0±0.1	24.0	1000	126.8±0.3	0.82±0.01	0.12	654

Table 1: L_α Caillé model fitting results for dilution along the 1.21 oct:SDS ratio. Constant parameters, δ_{head} = 3 Å, SLD_{brine} = 6.23 10^{-6} Å^{-2}, SLD_{tail} = -0.416 10^{-6} Å^{-2}, SLD_{head} = 1.7 10^{-6} Å^{-2}

T, °C	ϕ_v	I_{incoh}, cm^{-1}	scale	B	ξ_3, Å	δ_m, Å	ξ, Å	σ, Å	χ^2
35	0.189	0.121	0.03	3.1E-04	150.0±1.5	23.5±0.2	236.1±0.2	30.0±0.2	9150
	0.158	0.109	0.65	1.82E-04	117.8±0.4	24.3±0.1	253.2±0.1	34.9±0.1	854
	0.127	0.099	0.89	0.63E-04	150.3±0.3	24.1±0.1	276.1±0.2	51.8±0.1	94
	0.096	0.064	0.97	0.7E-04	174.2±0.3	24.5±0.1	387.7±0.2	61.7±0.1	88
	0.064	0.055	1.00	1.5E-04	175.6±0.3	23.9±0.1	658.9±0.2	62.6±0.1	112
45	0.189	0.121	0.91	2.6E-04	96.4±0.5	24.5±0.1	174.9±0.2	25.0±0.1	54
	0.158	0.109	0.98	1.3E-04	110.1±0.3	24.5±0.1	223.4±0.2	37.9±0.1	195
	0.127	0.099	0.85	1.6E-04	114.5±0.3	24.0±0.1	281.7±0.1	41.8±0.1	5
	0.096	0.064	0.75	1.5E-04	151.9±0.3	24.5±0.1	393.9±0.1	46.2±0.1	145
	0.064	0.055	0.70	1.8E-03	138.9±0.7	24.5±0.3	688.2±0.1	31.4±0.1	136

Table 2: L_3 model fitting results for dilution along the 1.21 oct:SDS ratio. Constant parameters, δ_{head} = 3.0 Å, A = 0.001, ξ_{io} = 1000 Å, $SLD_{contrast}$ = 5.9 10^{-6} Å^{-2}

T, °C	ϕ_v	I_{incoh}, cm^{-1}	scale	δ_{tail}, Å	δ_m, Å	N$_{layers}$	d, Å	η	p_D	χ^2
25	0.184	0.151	0.67	8.8±0.1	23.6	2000	120.3±0.6	0.88±0.01	0.11	422
	0.154	0.121	0.64	9.0±0.1	24.0	1000	137.0±0.9	0.99±0.02	0.12	436
	0.123	0.101	1.00	10.2±0.2	26.5	1000	171.0±1.7	1.00±0.02	0.21	452
35	0.184	0.151	0.72	8.3±0.1	22.5	5000	119.5±0.5	0.88±0.02	0.08	732
	0.154	0.121	0.51	10.5±0.1	27.0	1000	137.0±0.9	1.00±0.02	0.13	754
	0.123	0.101	1.0	10.2±0.2	26.4	1000	182.9±1.9	1.00±0.02	0.22	273
45	0.184	0.151	0.72	8.3±0.1	22.5	5000	119.0±0.5	0.85±0.04	0.08	452
	0.154	0.121	0.57	9.3±0.1	24.6	300	144.0±0.9	0.98±0.04	0.13	713
	0.123	0.101	1.005	10.4±0.1	26.7	1000	187.72±1.9	1.00±0.02	0.21	614
	0.093	0.065	1.00	10.0±0.6	25.9	1000	247.9±2.8	1.00±0.05	0.23	395

Table 3: L_α Caillé model with power law results for dilution along the 1.15 oct:SDS ratio. Constant parameters, δ_{head} = 3 Å, SLD_{brine} = 6.23 10^{-6} Å^{-2}, SLD_{tail} = -0.415 10^{-6} Å^{-2}, SLD_{head} = 1.74 10^{-6} Å^{-2}

T, °C	ϕ_v	I_{incoh}, cm^{-1}	scale	δ_{tail}, Å	δ_m, Å	N$_{layers}$	d, Å	η	p_D	χ^2
25	0.177	0.114	0.55	9.7±0.1	25.4	250	128.0±0.9	1.00±0.01	0.15	944
	0.148	0.107	0.44	11.5±0.1	28.9	500	151.0±1.9	1.00±0.01	0.26	1393
35	0.177	0.114	0.54	9.8±0.1	25.5	1000	128.4±0.9	1.00±0.01	0.15	563
	0.148	0.107	0.47	10.8±0.1	27.6	500	151.5±1.7	1.00±0.01	0.22	1219
45	0.177	0.114	0.54	9.7±0.1	25.4	3000	129.3±0.7	0.95±0.01	0.11	439
	0.148	0.107	0.52	10.0±0.1	26.0	500	152.5±1.2	0.99±0.01	0.16	1150

Table 4: L_α Caillé model fitting results for 1.08 oct:SDS ratio temperature scan. Constant parameters,δ_{head} = 3 Å, SLD_{brine} = 6.23 10^{-6} Å^{-2}, SLD_{tail} = -0.414 10^{-6} Å^{-2}, SLD_{head} = 1.81 10^{-6} Å^{-2}

T, °C	ϕ_v	I_{incoh}, cm^{-1}	d, Å	L, Å	L$_4$/L$_1$	χ^2
25	0.135	0.102	89.0±0.3	490±30	0.63	133
	0.113	0.095	105.2±0.3	309±35	2.22	245
	0.09	0.085	108.2±0.3	284±29	3.15	185
	0.068	0.067	111.1±0.3	291±40	4.28	134
	0.045	0.073	112.7±0.3	304±53	4.34	90
35	0.135	0.104	91.3±0.1	480±30	0.60	143
	0.113	0.092	106.9±0.4	330±28	2.31	231
	0.09	0.084	108.7±0.4	287±30	3.17	204
	0.068	0.067	112.9±0.4	303±42	4.48	140
	0.045	0.073	114.4±0.4	311±55	4.49	93
45	0.135	0.103	97.1±0.4	493±37	0.62	120
	0.113	0.091	112.4±0.4	402±37	2.23	267
	0.09	0.082	118.4±0.1	354±30	3.64	174
	0.068	0.065	120.5±0.1	391±72	5.16	95
	0.045	0.071	120.7±0.1	386±48	4.35	65

Table 5: L$_4$/L$_1$ lamellar + flexible cylinder fitting results for 0.62 oct:SDS ratio dilutions. Constant parameters, SLD_{brine} = 6.23 10^{-6} Å^{-2}, SLD_{head} = 2.2 10^{-6} Å^{-2}, SLD_{tail} = $-$0.45 10^{-6} Å^{-2}, scale = 0.25-0.4, l_{tail} = 9.5 Å, l_{head} = 3.0 Å, N_{layers} = 5, η = 1, b = 14 ±1 Å, R = 14±0.5 Å

T, °C	ϕ_v	scale	I_{incoh}, cm^{-1}	R, Å	L, Å	χ^2
25	0.085	0.09	0.07	15.6±0.2	54±10	40
	0.071	0.07	0.07	15.3 ±0.3	68±15	20
	0.057	0.05	0.06	14.8 ±0.3	150±20	34
	0.043	0.04	0.05	14.8 ±0.7	210±40	26
35	0.085	0.09	0.07	15.3±0.2	50±10	56
	0.071	0.07	0.07	15.0±0.3	62±15	108
	0.057	0.05	0.06	14.5±0.2	130±20	39
	0.043	0.04	0.05	14.5±0.4	170±20	24
45	0.085	0.09	0.07	14.8±0.1	45±10	113
	0.071	0.07	0.07	15.4±0.3	53±15	113
	0.057	0.05	0.06	14.2±0.2	115±40	113
	0.043	0.04	0.05	14.1±0.4	140±30	113

Table 6: L$_1$ fitting results for 0.08 oct:SDS ratio dilution. Constant parameters, δ_{shell} = 3 Å, SLD_{brine} = 5.7 10^{-6} Å^{-2}, SLD_{shell} = 3.0 10^{-6} Å^{-2}, SLD_{core} = $-$0.45 10^{-6} Å^{-2}

5 Temperature scan fitting results

T, °C	scale	δ_{tail}, Å	δ_m, Å	d, Å	η	p_D	χ^2
25	0.65	9.2±0.1	24.4	137.0±0.3	1.00±0.01	0.12	654
30	0.64	8.9±0.1	23.9	137.0±0.3	1.00±0.07	0.11	718
35	0.32	9.2±0.1	24.5	137.0±0.2	1.00±0.06	0.06	475

Table 7: L_α Caillé model fitting results for 1.21 oct:SDS ratio temperature scan. Constant parameters, I_{incoh} = 0.109, δ_{head} = 3 Å, N$_{layers}$ = 50

T, °C	scale	B	ξ_3, Å	δ_m, Å	ξ, Å	σ, Å	χ^2
35	0.68	4.6E-05	194.0±1.5	26.0±0.2	243.4±0.2	42.7±0.2	604
40	1.45	1.0E-04	114.9±0.4	27.0±0.1	219.2±0.1	39.8±0.1	234
45	1.47	1.4E-04	100.9±0.3	25.5±0.1	219.0±0.2	40.1±0.1	281
50	1.48	1.4E-04	97.0±0.3	25.3±0.1	215.3±0.2	40.7±0.1	252
55	1.52	1.4E-04	94.0±0.3	25.1±0.1	208.7±0.2	40.4±0.1	386
60	1.56	1.4E-04	91.0±0.3	25.9±0.1	202.0±0.1	40.0±0.1	570
65	1.56	1.5E-04	87.2±0.3	25.9±0.1	195.3±0.1	39.2±0.1	729
25	1.26	4.6E-5	151.1±0.7	25.5±0.0	237.3±0.1	49.6±0.1	552

Table 8: L_3 model fitting results for 1.21 oct:SDS ratio temperature scan. Constant parameters, I_{incoh} = 0.12, δ_{head} = 3 Å, N$_{layers}$ = 50

T, °C	scale	δ_{tail}, Å	δ_m, Å	d, Å	η	p_D	χ^2
25	0.86	10.2±0.3	26.3	137.0±3.0	1.00±0.02	0.14	263
30	0.86	10.2±0.3	26.3	137.0±3.0	1.00±0.02	0.14	306
35	0.87	10.2±0.3	26.4	137.0±3.0	1.00±0.02	0.13	604
40	1.00	9.4±0.3	24.9	142.1±3.0	1.00±0.02	0.13	234
45	0.98	9.2±0.3	24.4	144.2±3.0	0.99±0.01	0.12	281
50	0.99	9.0±0.3	24.1	145.6±3.0	0.97±0.02	0.12	252
55	0.90	8.9±0.3	23.7	146.2±2.0	0.98±0.02	0.11	386
60	0.99	8.7±0.3	23.4	146.7±2.0	0.98±0.02	0.11	570
65	0.90	8.5±0.3	23.0	148.4±2.0	0.90±0.01	0.12	729
25	0.99	9.3±0.3	24.5	150.0±1.0	0.98±0.01	0.12	552

Table 9: L_α Caillé model fitting results for 1.15 oct:SDS ratio temperature scan. Parameters have been kept constant I_{incoh} = 0.12, δ_{head} = 3 Å, N$_{layers}$ = 50

T, °C	scale	δ_{tail}, Å	δ_m, Å	d, Å	η	p_D	χ^2
25	0.47	10.5±0.2	27.0	152.9±0.6	1.00±0.02	0.24	184
30	0.50	10.1±0.2	26.2	153.6±0.5	1.00±0.02	0.22	169
35	0.53	9.7±0.1	25.3	154.2±0.4	1.00±0.01	0.18	224
40	0.55	9.3±0.1	24.6	154.5±0.4	1.00±0.01	0.15	201
45	0.56	9.1±0.1	24.2	155.0±0.3	1.00±0.01	0.13	252
50	0.56	8.9±0.1	23.8	155.4±0.4	1.00±0.02	0.12	284
55	0.56	8.7±0.1	23.3	156.5±0.3	0.99±0.02	0.11	429
60	0.56	8.5±0.1	23.0	157.0±0.4	0.98±0.02	0.11	585
65	0.55	8.4±0.1	22.9	157.1±0.4	0.97±0.01	0.11	641
25	0.50	9.4±0.1	24.7	160.0±0.4	1.00±0.01	0.13	625

Table 10: L_α Caillé model fitting results for 1.08 oct:SDS ratio temperature scan. Constant parameters, I_{incoh} = 0.11, δ_{head} = 3 Å, N_{layers} = 20,

T, °C	d, Å	L, Å	L_4/L_1	χ^2
25	13.6±0.1	309±25	2.22	245
30	105.2±0.2	329±28	2.37	333
35	107.1±0.2	330±28	2.31	231
40	106.9±0.2	331±27	2.05	235
45	106.6±0.3	402±35	2.23	267
50	112.4±0.3	493±43	2.12	242
55	118.3±0.3	654±18	1.55	258
60	119.4±0.4	846±71	1.29	224
65	142.7±0.6	1008±86	1.02	227
25	157.2±0.7	1213±108	1.29	194

Table 11: L_4-L_1 fitting results for 0.62 oct:SDS ratio temperature scan. Constant parameters, I_{incoh} = 0.86-0.89 cm^{-1}, SLD_{brine} = 6.23 10^{-6} $Å^{-2}$

T, °C	R, Å	L, Å	χ^2
25	15.2±0.3	67.9±20	19
30	15.7±0.3	61.6±20	20
35	15.0±0.3	61.8±18	19
40	14.9±0.3	58.8±15	19
45	15.4±0.3	53.4±14	111
50	15.3±0.3	51.2±12	109
55	15.2±0.3	48.9±10	108
60	15.0±0.3	46.7±8	110
65	14.9±0.3	44.6±6	113
25	15.8±0.3	65.8±20	135

Table 12: L_1 fitting results for 0.08 oct:SDS ratio temperature scan. Constant parameters, scale = 0.068-0.070 I_{incoh} = 0.067-0.069 cm^{-1}, δ_{shell} = 3 Å, SLD_{brine} = 5.7 10^{-6} $Å^{-2}$, SLD_{shell} = 3.0 10^{-6} $Å^{-2}$, SLD_{core} = -0.45 10^{-6} $Å^{-2}$

References

[1] N. Lei, C. R. Safinya, D. Roux, and K. S. Liang. Phys. Rev. E 56(1), 608 - 613 (1997).
[2] L. Porcar, W. A. Hamilton, P. D. Butler, and G. G. Warr. Langmuir 19(26), 10779 - 10794 (2003).
[3] F. Nallet, R. Laversanne, and D. Roux. J. Phys. II France 3, 487-502 (1993).
[4] C. G. Malmberg and A. A. Maryott. J Res Natl Inst Stand Technol 56(I), Paper 2641 (1956).
[5] N. Gavish and K. Promislow. Phys. Rev. E 94, 012611 (2016).
[6] L.A. Feigin and D.I. Svergun. Vol.1 Springer (1987).
[7] S. R. Kline. J Appl. Cryst. 39, 895 (2006).